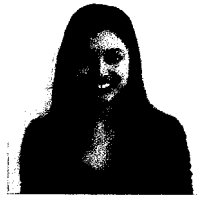


INDIRECT SEARCHES FOR STERILE NEUTRINOS AT A HIGH-LUMINOSITY Z -FACTORY

VALENTINA DE ROMERI^a

*Laboratoire de Physique Corpusculaire, CNRS/IN2P3 – UMR 6533,
Campus des Cézeaux, 24 Av. des Landais, F-63177 Aubière Cedex, France*



A future high-luminosity Z -factory has the potential to investigate lepton flavour violation. Rare decays such as $Z \rightarrow \ell_1^{\mp} \ell_2^{\pm}$ are potentially complementary to low-energy (high-intensity) observables of lepton flavour violation. Here we consider two extensions of the Standard Model which add to its particle content one or more sterile neutrinos. We address the impact of the sterile fermions on lepton flavour violating Z decays, focusing on potential searches at FCC-ee (TLEP), and taking into account experimental and observational constraints. We show that sterile neutrinos can give rise to contributions to $\text{BR}(Z \rightarrow \ell_1^{\mp} \ell_2^{\pm})$ within reach of the FCC-ee. We discuss the complementarity between a high-luminosity Z -factory and low-energy charged lepton flavour violation facilities.

1 Introduction

Despite the recent experimental advances, the neutrino physics picture is still incomplete. Among the missing ingredients are the CP-violating phase(s), the mass ordering (normal (NH) or inverted (IH) hierarchy) and the absolute mass scale. Moreover, it remains to clarify whether neutrinos are Majorana or Dirac particles, and to understand what is the underlying mechanism responsible for the generation of their masses. Several frameworks which account for neutrino masses and mixings are extensions of the Standard Model (SM) which introduce sterile neutrinos. These models are further motivated by anomalous experimental results (see [1] and references therein), as well as by certain indications from large scale structure formation [1, 2].

The existence of sterile neutrinos may be investigated at colliders: for instance, the case for a high luminosity circular e^+e^- collider (called FCC-ee), operating at centre-of-mass energies ranging from the Z pole up to the top quark pair threshold is being actively studied [3]. Its characteristics should allow to obtain a typical peak luminosity at the Z pole of $\sim 10^{36} \text{ cm}^{-2} \text{ s}^{-1}$. A year of operation at the Z pole centre-of-mass energy would then yield $\sim 10^{12}$ Z boson decays to be recorded. Motivated by the design study for such a powerful machine, we have investigated the prospects for indirect searches for sterile neutrinos by means of rare *charged* lepton flavour violating (cLFV) Z decays [4].

^abased on a work done in collaboration with A. ABADA, S. MONTEIL, J. ORLOFF and A. M. TEIXEIRA

2 Leptonic Z decays in the presence of sterile neutrinos

Lepton-flavour changing Z decays are forbidden in the SM due to the GIM mechanism [5], and their rates remain extremely small ($\sim 10^{-54} - 10^{-60}$) even when lepton mixing is introduced. The observation of such a rare decay would therefore serve as an indisputable evidence of new physics [6–13]. We consider here two extensions of the SM which introduce sterile fermions. The mixing in the neutral lepton sector induced by these Majorana states also opens the possibility for flavour violation in $Z\nu_i\nu_j$ interactions (flavour-changing neutral currents), coupling both the left- and right-handed components of the neutral fermions to the Z boson. Together with the charged-current LFV couplings, these interactions will induce an effective cLFV vertex $Z\ell_1^{\mp}\ell_2^{\pm}$.

3 Extensions of the SM by sterile neutrinos

The effective “3+1 toy model” A simple approach to address the impact of sterile fermions on rare cLFV Z decays consists in considering a minimal model where only one sterile Majorana state is added to the three light active neutrinos of the SM. This allows for a first, generic, evaluation of the impact of the sterile fermions for these processes. In this simple toy model, no assumption is made on the underlying mechanism of neutrino mass generation. The addition of an extra neutral fermion to the particle content translates into extra degrees of freedom: the mass of the new sterile state, m_4 , three active-sterile mixing angles θ_{i4} , two new (Dirac) CP phases and one extra Majorana phase. This leads to the definition of a 4×4 mixing matrix U_{ij} , whose 3×4 sub-matrix U_{lj} appears in the SM charged-currents Lagrangian (see Eq. (4) below). In our analysis, and for both NH and IH light neutrino spectra, we scan over the following range for the sterile neutrino mass: $10^{-9} \text{ GeV} \lesssim m_4 \lesssim 10^6 \text{ GeV}$, while the active-sterile mixing angles are randomly varied in the interval $[0, 2\pi]$ ^b. All CP phases are also taken into account, and likewise randomly varied between 0 and 2π .

The Inverse Seesaw framework The Inverse Seesaw (ISS) mechanism [14] is an example of (type I) low-scale seesaw realisation which in full generality calls upon the introduction of at least two generations of SM singlets. Here, we consider the addition of three generations of right-handed neutrinos ν_R and of extra $SU(2)$ singlets fermions X to the SM particle content. Both ν_R and X carry lepton number $L = +1$ [14]. The SM Lagrangian is thus extended as $\mathcal{L}_{\text{ISS}} = \mathcal{L}_{\text{SM}} - Y_{ij}^\nu \bar{\nu}_{Ri} \tilde{H}^\dagger L_j - M_{Rij} \bar{\nu}_{Ri} X_j - \frac{1}{2} \mu_{Xij} \bar{X}_i^c X_j + \text{h.c.}$, where $i, j = 1, 2, 3$ are generation indices and $\tilde{H} = i\sigma_2 H^*$. Lepton number $U(1)_L$ is broken only by the non-zero Majorana mass term μ_X , while the Dirac-type RH neutrino mass term M_R does conserve lepton number. In the $(\nu_L, \nu_R^c, X)^T$ basis, and after EW symmetry breaking, the (symmetric) 9×9 neutrino mass matrix \mathcal{M} is given by

$$\mathcal{M} = \begin{pmatrix} 0 & m_D^T & 0 \\ m_D & 0 & M_R \\ 0 & M_R^T & \mu_X \end{pmatrix}, \quad (1)$$

with $m_D = Y^\nu v$ the Dirac mass term, v being the vacuum expectation value of the SM Higgs boson. Under the assumption that $\mu_X \ll m_D \ll M_R$, the diagonalization of \mathcal{M} leads to an effective Majorana mass matrix for the active (light) neutrinos [15],

$$m_\nu \simeq m_D^T M_R^{T^{-1}} \mu_X M_R^{-1} m_D. \quad (2)$$

The remaining six (mostly) sterile states form nearly degenerate pseudo-Dirac pairs, with masses

$$m_{S\pm} = \pm \sqrt{M_R^2 + m_D^2} + \frac{M_R^2 \mu_X}{2(m_D^2 + M_R^2)}. \quad (3)$$

^bWe always ensure that the perturbative unitary bound on the sterile masses and their couplings to the active states is respected.

In the ISS, the full neutrino mass matrix is diagonalised by a 9×9 unitary mixing matrix \mathbf{U} as $\mathbf{U}^T \mathcal{M} \mathbf{U} = \text{diag}(m_i)$. In the basis where the charged lepton mass matrix is diagonal, the leptonic mixing matrix \mathbf{U} (see Eq. (4) below) is given by the rectangular 3×9 sub-matrix corresponding to the first three columns of \mathbf{U} . This framework is phenomenologically appealing because it allows to accommodate neutrino data with natural values of the Yukawa couplings, while at the same time comparatively light sterile neutrino masses are possible. The possibility of having sizeable mixings between the active and sterile states, will have a non-negligible impact for several observables.

4 Constraints on sterile neutrino extensions of the SM

The introduction of sterile fermion states, which have a non-vanishing mixing to the active neutrinos, leads to a modification of the leptonic charged current Lagrangian:

$$-\mathcal{L}_{cc} = \frac{g}{\sqrt{2}} \mathbf{U}^{ji} \bar{\ell}_j \gamma^\mu P_L \nu_i W_\mu^- + \text{c.c.}, \quad (4)$$

where \mathbf{U} is the leptonic mixing matrix, $i = 1, \dots, n_\nu$ denotes the physical neutrino states and $j = 1, \dots, 3$ the flavour of the charged leptons. In the standard case of three neutrino generations, \mathbf{U} corresponds to the unitary matrix U_{PMNS} . For $n_\nu > 3$, the mixing between the left-handed leptons, which we denote by \tilde{U}_{PMNS} , corresponds to a 3×3 sub-block of \mathbf{U} , which can show some deviations from unitarity. One can parametrise [16] the \tilde{U}_{PMNS} mixing matrix as $U_{\text{PMNS}} \rightarrow \tilde{U}_{\text{PMNS}} = (1 - \eta) U_{\text{PMNS}}$, where the matrix η encodes the deviation of the \tilde{U}_{PMNS} from unitarity [17, 18], due to the presence of extra neutral fermion states. One can also introduce the invariant quantity $\tilde{\eta}$, defined as

$$\tilde{\eta} = 1 - |\text{Det}(\tilde{U}_{\text{PMNS}})|, \quad (5)$$

particularly useful to illustrate the effect of the new active-sterile mixings (corresponding to a deviation from unitarity of the \tilde{U}_{PMNS}) on several observables.

The deviation from unitarity of \mathbf{U} will induce a departure from the SM expected values of several observables. In turn, this is translated into a vast array of constraints which we will apply to our analysis (see details and references in [4]):

- **Neutrino oscillation data** The most important constraint on any model of massive neutrinos is to comply with ν -oscillation data. We impose neutrino oscillation parameters from [19], for both NH and IH of the light neutrino spectrum.
- **Perturbativity** Although no upper limit on the mass of the heavy neutrinos exists, the decay of the (mostly) sterile heavy states should comply with the perturbative unitary condition $\frac{\Gamma_{\nu_i}}{m_{\nu_i}} < \frac{1}{2}$ ($i \geq 4$), which translates into a bound on sterile neutrino masses.
- **Unitarity constraints** Non-standard neutrino interactions with matter can be generated by the introduction of fermionic sterile states. We consider the constraints on the non-unitarity matrix η from [20, 21], for sterile neutrino masses in the range $\text{GeV} \lesssim m_\nu \lesssim \Lambda_{\text{EW}}$, being Λ_{EW} the electroweak scale.
- **Electroweak precision data** The addition of sterile states to the SM, with a sizeable active-sterile mixing, may have an impact on electroweak precision observables either at tree-level (charged currents) or at higher order. We apply these bounds to our analysis and we further require that the new contributions to the cLFV Z decay width do not exceed the present uncertainty on the total Z width.
- **LHC constraints** LHC data constrain parts of the parameter space where the sterile neutrinos are lighter than the Higgs boson, through searches for Higgs decays to an active neutrino and a heavier (mostly) sterile one.

- **Leptonic and semileptonic meson decays** Further constraints arise from leptonic and semileptonic decays of pseudoscalar mesons, as for example K , D , D_s , B .
- **Laboratory searches** Negative searches for monochromatic lines in the spectrum of muons from $\pi^\pm \rightarrow \mu^\pm \nu$ decays also impose robust bounds on sterile neutrino masses in the MeV-GeV range.
- **Neutrinoless double beta decay** The introduction of Majorana sterile neutrinos allows for processes which violate lepton number, such as $0\nu2\beta$ decay. The sensitivities of current experiments put a limit on the effective neutrino Majorana mass - to which the amplitude of $0\nu2\beta$ process is proportional - in the range $|m_{ee}| \lesssim 140$ meV – 700 meV.
- **Lepton flavour violation** The sterile fermions will contribute to several charged lepton flavour violating processes such as $\ell \rightarrow \ell' \gamma$, $\ell \rightarrow \ell_1 \ell_1 \ell_2$ and $\mu - e$ conversion in muonic atoms, the rates depending on their masses and mixings with the active neutrinos. In our analysis we compute the contribution of the sterile states to all these observables, imposing compatibility with current experimental bounds and considering the impact of future experimental sensitivities.
- **Cosmological bounds** Several cosmological observations (CMB, Lyman- α , X-rays, clusters, etc...) put severe constraints on sterile neutrinos with a mass below the TeV. However, these bounds are derived assuming a standard cosmology; the possibility of a non-standard cosmology could allow to evade some of the above bounds. Aiming at conservativity, we will allow for the violation of these cosmological bounds in some scenarios.

5 Results

We proceed to discuss the impact of the additional sterile states on cLFV Z decays for the two scenarios discussed in Section 3.

cLFV Z decays in the “3+1 model”

This minimal extension of the SM by one sterile neutrino can account for values of $\text{BR}(Z \rightarrow \ell_1^\mp \ell_2^\pm)$ within the sensitivity of a high luminosity Z -factory, such as the FCC-ee. Nevertheless, the largest cLFV Z decay branching fractions (as large as $\mathcal{O}(10^{-6})$) cannot be reconciled with current bounds on low-energy cLFV processes. Indeed, sterile neutrinos also contribute via Z penguin diagrams to cLFV 3-body decays and $\mu - e$ conversion in nuclei, which severely constrain the flavour violating $Z \ell_1^\mp \ell_2^\pm$ vertex (see also [10–12]). Moreover, the recent MEG result on $\mu \rightarrow e\gamma$ also excludes important regions of the parameter space. These constraints are especially manifest in the case of $Z \rightarrow e\mu$ decays, since the severe limits from $\text{BR}(\mu \rightarrow 3e)$ and $\text{CR}(\mu - e, \text{Au})$ typically preclude $\text{BR}(Z \rightarrow e\mu) \gtrsim 10^{-13}$.

In Fig. 1 we illustrate the complementary rôle of a high-luminosity Z -factory with respect to low-energy (high-intensity) cLFV dedicated experiments. We display the sterile neutrino contributions to $\text{BR}(Z \rightarrow \ell_1^\mp \ell_2^\pm)$ versus two different low-energy cLFV observables: $\text{CR}(\mu - e, \text{Al})$ and $\text{BR}(\tau \rightarrow \mu\gamma)$. In the plots, we identify as grey points the solutions which fail to comply with (at least) one of the constraints listed in Section 4. We depict in red the points that survive all other bounds but are typically disfavoured from standard cosmology arguments. Finally, blue points are in agreement with *all* imposed constraints. We further highlight in dark yellow solutions which allow for a third complementary observable within future sensitivity, which is the effective neutrino mass in $0\nu2\beta$ decays. As can be inferred from Fig. 1, low-energy cLFV dedicated facilities offer much better prospects to probe lepton flavour violation in the $\mu - e$ sector of the “3+1 model” than a high-luminosity Z -factory. In particular, Mu3e (PSI) [22] and COMET (J-PARC) [23] will be sensitive to regions in parameter space associated with $\text{BR}(Z \rightarrow e\mu) \sim 10^{-17 \div -13}$, beyond the reach of FCC-ee. Interestingly, the situation is reversed for the case of the $\mu - \tau$ sector. Moreover, a non negligible subset of the parameter space is testable at a third type of facilities, through

$0\nu2\beta$ decay searches (especially in the case of an IH light neutrino spectrum, although we have not displayed it here).

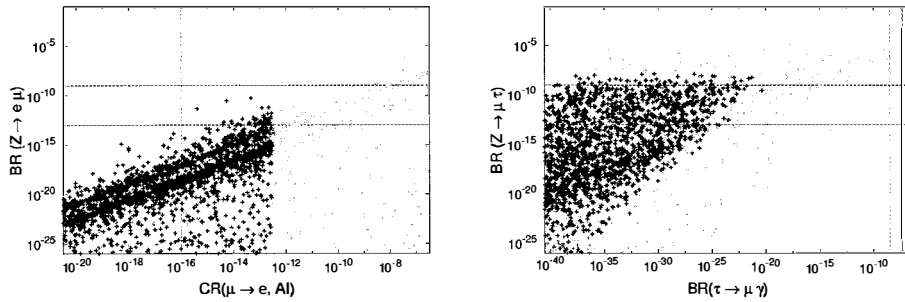


Figure 1 – The “3+1 model”: on the left, $\text{BR}(Z \rightarrow e\mu)$ versus $\text{CR}(\mu \rightarrow e, \text{Al})$, and $\text{BR}(Z \rightarrow \mu\tau)$ vs $\text{BR}(\tau \rightarrow \mu\gamma)$ on the right, for a NH light neutrino spectrum (IH leads to similar results). See text for the description of the color code. When present, the additional green vertical lines denote the current bounds (solid) and future sensitivity (dashed), and dark-yellow points denote an associated $|m_{ee}|$ within experimental reach.

cLFV Z decays in the ISS

We show the results for this well motivated framework of neutrino mass generation in Fig. 2. On the left, we show the $\text{BR}(Z \rightarrow \mu\tau)$ as a function of the average of the absolute masses of the mostly sterile states, $\langle m_{4-9} \rangle = \sum_{i=4-9} \frac{1}{6} |m_i|$ (same color code as in Fig. 1). These results indicate that this ISS realisation can account for sizeable values of cLFV Z -decay branching ratios, at least for the second and third generations of leptons. This in general requires sterile states with a mass $\gtrsim \Lambda_{\text{EW}}$, and can occur even for very mild deviations from unitarity of the \tilde{U}_{PMNS} . Other cLFV decays, $Z \rightarrow e\mu$ and $Z \rightarrow e\tau$ have BRs $\lesssim \mathcal{O}(10^{-11})$, but still within experimental sensitivity. The prospects for the observation of cLFV Z decays in this framework are summarised in the right plot of Fig. 1 by considering the values of $\text{BR}(Z \rightarrow \ell_1^\mp \ell_2^\pm)$ in the $(\tilde{\eta}, \langle m_{4-9} \rangle)$ parameter space of this specific realisation and for a NH light neutrino spectrum. We denote the values of the BRs from larger (dark blue) to smaller (orange); cyan denotes values of the branching fractions below 10^{-18} . As to the complementarity of low-energy cLFV observables and cLFV Z decays at a high-luminosity Z factory, the results (which are not shown here) are in agreement with the findings for the “3+1 model”. Low-energy experiments - as COMET looking for $\mu - e$ conversion in Al nuclei - are better probes of cLFV in the $\mu - e$ sector of this ISS realisation; on the other hand, a future high-luminosity Z factory has a stronger power to probe lepton flavour violation in the $\mu - \tau$ sector via Z decays.

6 Conclusions

We have considered two extensions of the SM which add to its particle content one or more sterile neutrinos. We have explored indirect searches for these sterile states at a future circular collider like FCC-ee, running close to the Z mass threshold. We have considered the contribution of the sterile states to rare cLFV Z decays in these two classes of models and discussed them taking into account a number of experimental and theoretical constraints. Among these, low-energy LFV observables like cLFV 3-body decays and $\mu - e$ conversion in nuclei impose strong constraints on the sterile neutrino induced $\text{BR}(Z \rightarrow \ell_1^\mp \ell_2^\pm)$. Our analysis emphasises the underlying synergy between a high-luminosity Z factory and dedicated low-energy facilities: regions of the parameter space of both models can be probed via LFV Z decays at FCC-ee, at low-energy cLFV dedicated facilities and also via searches for $0\nu2\beta$. Notably, FCC-ee could better probe LFV in the $\mu - \tau$ sector, in complementarity to the reach of low-energy experiments like COMET.

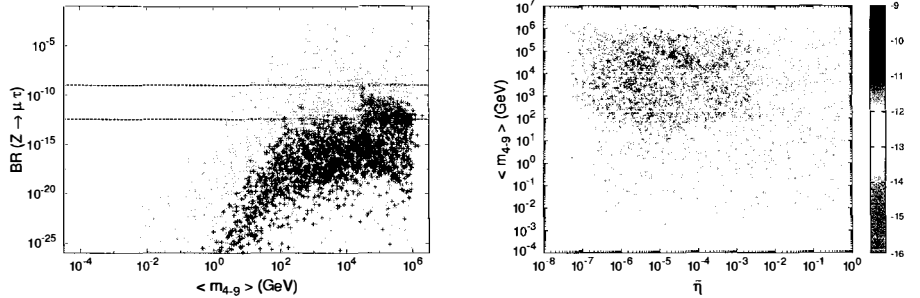


Figure 2 – ISS realisation: $\text{BR}(Z \rightarrow \mu\tau)$ as a function of the average value of the mostly sterile state masses (right), $\langle m_{4-9} \rangle$, for a NH light neutrino spectrum (left); maximal values (in log scale) of $\text{BR}(Z \rightarrow \ell_1^\mp \ell_2^\pm)$ on the $(\bar{\eta}, \langle m_{4-9} \rangle)$ parameter space (right) for a NH light neutrino spectrum, from larger (dark blue) to smaller (orange) values. Cyan denotes values of the branching fractions below 10^{-18} .

Acknowledgments

VDR is grateful to the organisers of the Moriond 2015 EW session for the invitation and for the financial support. The research of VDR is supported by the European Union FP7 ITN INVISIBLES (Marie Curie Actions, PITN-GA-2011-289442).

References

1. K. N. Abazajian *et al.*, arXiv:1204.5379 [hep-ph].
2. A. Kusenko, Phys. Rept. **481** (2009) 1 [arXiv:0906.2968 [hep-ph]].
3. M. Bicer *et al.*, JHEP **1401** (2014) 164 [arXiv:1308.6176 [hep-ex]].
4. A. Abada, V. De Romeri, S. Monteil, J. Orloff and A. M. Teixeira, JHEP **1504** (2015) 051 [arXiv:1412.6322 [hep-ph]].
5. S. L. Glashow *et al.*, Phys. Rev. D **2** (1970) 1285.
6. G. Mann and T. Riemann, Annalen Phys. **40** (1984) 334.
7. J. I. Illana *et al.*, in *2nd ECFA/DESY Study 1998-2001*, 490-524 [hep-ph/0001273].
8. J. I. Illana and T. Riemann, Phys. Rev. D **63** (2001) 053004 [hep-ph/0010193].
9. A. Ilakovac and A. Pilaftsis, Nucl. Phys. B **437** (1995) 491 [hep-ph/9403398].
10. M. A. Perez *et al.*, Int. J. Mod. Phys. A **19** (2004) 159 [hep-ph/0305227].
11. A. Flores-Thlalpa *et al.*, Phys. Rev. D **65** (2002) 073010 [hep-ph/0112065].
12. D. Delepine and F. Vissani, Phys. Lett. B **522** (2001) 95 [hep-ph/0106287].
13. S. Davidson, S. Lacroix and P. Verdier, JHEP **1209** (2012) 092 [arXiv:1207.4894 [hep-ph]].
14. R. N. Mohapatra and J. W. F. Valle, Phys. Rev. D **34** (1986) 1642.
15. M. C. Gonzalez-Garcia and J. W. F. Valle, Phys. Lett. B **216** (1989) 360.
16. E. Fernandez-Martinez *et al.*, Phys. Lett. B **649** (2007) 427 [hep-ph/0703098].
17. J. Schechter and J. W. F. Valle, Phys. Rev. D **22** (1980) 2227.
18. M. Gronau, C. N. Leung and J. L. Rosner, Phys. Rev. D **29** (1984) 2539.
19. D. V. Forero, M. Tortola and J. W. F. Valle, Phys. Rev. D **90** (2014) 093006 [arXiv:1405.7540 [hep-ph]].
20. S. Antusch, J. P. Baumann and E. Fernandez-Martinez, Nucl. Phys. B **810** (2009) 369 [arXiv:0807.1003 [hep-ph]].
21. S. Antusch and O. Fischer, JHEP **1410** (2014) 94 [arXiv:1407.6607 [hep-ph]].
22. A. Blondel *et al.*, arXiv:1301.6113 [physics.ins-det].
23. Y. Kuno [COMET Collaboration], PTEP **2013** (2013) 022C01.